Published in final edited form as:
Brain Res. 2014 July 7; 1571: 49–60. doi:10.1016/j.brainres.2014.05.009.

In vivo measures of nigrostriatal neuronal response to unilateral MPTP treatment

LinLin Tian[a,#], **Morvarid Karimi**[a,#], **Chris A Brown**[a], **Susan K Loftin**[a], and **Joel S Perlmutter**[a,b,c,d,e]

[a]Neurology, Washington University, St. Louis, MO 63110, USA

[b]Radiology, Washington University, St. Louis, MO 63110, USA

[c]Neurobiology, Washington University, St. Louis, MO 63110, USA

[d]Occupational Therapy, Washington University, St. Louis, MO 63110, USA

[e]Physical Therapy, Washington University, St. Louis, MO 63110, USA

Abstract

A single unilateral intracarotid infusion of 1-methyl-4-phenyl-1,2,3,6-tetrahydropyridine (MPTP) into non-human primates causes injury to the nigrostriatal pathway including nigral cell bodies, axons and striatal terminal fields. In this model, motor parkinsonism correlates well with the loss of nigral dopaminergic cell bodies but only correlates with *in vitro* measures of nigrostriatal terminal fields when nigral cell loss does not exceed 50%. The goals of this study are to determine the relationship of motor parkinsonism with the degree of injury to nigrostriatal axons, as reflected by *in vitro* fiber length density measures, and compare *in vivo* with *in vitro* measures of striatal terminal fields. We determined axon integrity by measuring fiber length density with tyrosine hydroxylase (TH) immunohistology and dopamine transporter (DAT) density with DAT immunohistology. We then calculated the terminal arbor size and compared these measures with previously published data of quantified *in vivo* positron emission tomography (PET) measures of presynaptic dopaminergic neurons, autoradiographic measures of DAT and vesicular monoamine transporter type 2 (VMAT2), striatal dopamine, nigral cell counts, and parkinsonian motor ratings in the same animals. Our data demonstrate that *in vivo* and *in vitro* measures of striatal terminal fields correlate with each other regardless of the method of measurement. PET-based *in vivo* striatal measures accurately reflect *in vitro* measures of DAT and VMAT2. Terminal arbor size and other terminal field measures correlate with nigral TH immunoreactive (TH-ir) cell counts only when nigral TH-ir cell loss does not exceed 50%. Fiber length density was the only striatal measure that linearly correlated with motor ratings (Spearman: $r = -0.81$, $p < 0.001$, $n = 16$).

Correspondence: Joel S Perlmutter, 660 S. Euclid, Campus Box 8111, St. Louis, MO 63110-1093, Fax: (314) 362-0168, Telephone: (314) 362-6026, joel@npg.wustl.edu.
[#]These authors contributed equally to this work.

Keywords

Nigrostriatal; MPTP; Striatal terminal field; PET

1. Introduction

A single unilateral intracarotid infusion of 1-methyl-4-phenyl-1,2,3,6-tetrahydropyridine (MPTP) into non-human primates causes injury to the nigrostriatal pathway including nigral cell bodies, axons and striatal terminal fields that can cause stable hemiparkinsonism (Bankiewicz et al., 1986; Joyce et al., 1986; Palombo et al., 1990; Tabbal et al., 2006; Perlmutter et al., 1997). This animal model permits development and validation of neuroimaging biomarkers that may be useful for investigating humans with disorders such as Parkinson disease (PD). In particular this model permits comparisons of motor parkinsonism with the degree of injury to specific components of the nigrostriatal pathway. This may be important as the degree of nigral cell body injury may not correspond with the degree of striatal terminal field injury. For example, various parts of nigrostriatal pathway in PD patients are differentially involved (Burke and O'Malley, 2013; Kordower et al., 2013). In addition, in nonhuman primates given varying doses of intracarotid MPTP, motor parkinsonism correlates well with the loss of nigral dopaminergic cell bodies (Tabbal et al., 2012) but only correlates with measures of nigrostriatal terminal fields when nigral cell loss does not exceed 50%. Striatal measures in those studies included dopamine concentration (Tabbal et al., 2012) and striatal uptake of three classes of radiotracers targeting presynaptic dopaminergic neurons commonly used in positron emission tomography (PET) (Karimi et al., 2013). The goals of this study are to determine the relationship of motor parkinsonism with the degree of injury to nigrostriatal axons, as reflected by *in vitro* fiber length density and dopamine transporter (DAT) varicosity density in striatum, and compare *in vivo* with *in vitro* measures of striatal terminal fields.

We used this MPTP animal model to quantify the striatal response with *in vitro* tyrosine hydroxylase (TH) immunoreactive (ir) fiber length density, DAT varicosity density and terminal arbor size. These newly measured variables were compared with previously published data from the same animals of *in vivo* PET, quantified autoradiography, striatal dopamine, nigral cell counts and motor ratings of parkinsonism (Brown et al., 2012; Karimi et al., 2013; Tabbal et al., 2012; Tian et al., 2012). This allows us to investigate whether the measures of axonal fibers fall in between the striatal terminal field and nigral cell body measures in relative to motor parkinsonism.

2. Results

All 16 monkeys completed the study successfully with a range of motor impairment. One monkey was excluded from cell count analyses due to extensive damage to the midbrain tissue during processing procedures. Coefficients of error and coefficients of variance, calculated as estimates of precision, for TH measures in striatum and nigra as well as DAT measures in striatum were all < 0.1.

In vivo PET data had a tight correlation with corresponding *in vitro* measures. The nondisplaceable binding potential (BP_{ND}) of 2-beta-[^{11}C]carbomethoxy-3-beta-4-fluorophenyltropane (CFT; reflects DAT) tightly correlated with the maximum number of binding sites (Bmax) of DAT as both drop markedly and remain low once nigral cell loss exceeds 50% (Spearman: r = 0.95, $p < 0.001$, n = 16) (Fig 1 A). Similarly, striatal BP_{ND} of [^{11}C]dihydrotetrabenazine (DTBZ; reflects vesicular monoamine transporter type 2, VMAT2) correlated strongly with VMAT2 Bmax (Spearman: r = 0.90, $p < 0.001$, n = 16) (Fig 1B). We repeated the above correlation analyses selecting only a single point from the clustered data to ensure that the correlations were not driven by these clustered points (Spearman: $r = 0.88$, $p < 0.001$; r = 0.86, $p < 0.001$, respectively; $n = 10$).

DAT immunhistochemistry was performed to label dopaminergic terminals; the data presented in Fig. 2 A and B show brain sections from post-commissural striatum that were immunostained with DAT from both unlesioned and lesioned side. DAT density correlated with other striatal terminal field measures including CFT BP_{ND}, DTBZ BP_{ND} and influx constant (K_{occ}) for 6-[^{18}F]fluorodopa (FD; primarily reflects decarboxylase activity), striatal dopamine, quantitative autoradiographic measures of DAT Bmax and VMAT2 Bmax (Spearman: r = 0.90, r = 0.92, r = 0.92, r = 0.88, r = 0.9, r = 0.82, respectively, $p < 0.001$, n = 16) (Fig 3 A–F). Note, that all correlations remained significant when including only a single point in the lower left part of the graphs (see legends of figure 3).

Striatal terminal arbor size correlated with nigral cell count as long as cell loss did not exceed 50% (Spearman: r = 0.6, $p = 0.07$, n = 10). Once nigral cell loss exceeded 50%, terminal arbor size reached a nadir with a flooring effect (Fig 4 A). Striatal terminal arbor size also correlated with CFT BP_{ND}, DTBZ BP_{ND} and FD K_{occ}, striatal dopamine, DAT Bmax, and VMAT2 Bmax (Spearman: r = 0.88, r = 0.88, r = 0.89, r = 0.88, r = 0.89, r = 0.85, respectively, $p < 0.0001$, n = 15) (Fig 4 B–G). Note, that all correlations remained significant when including only a single point in the lower left part of the graphs (see legends of figure 4).

TH immunhistochemistry was performed to label striatal fibers; the data presented in Fig. 5 A and B show brain sections from post-commissural striatum that were immunostained with TH from both unlesioned and lesioned side. The fiber length density was a measure of axonal integrity and had a dichotomous relationship with *in vitro* or *in vivo* striatal terminal field measures (CFT BP_{ND}, DTBZ BP_{ND} and FD K_{occ}, striatal dopamine, DAT Bmax, and VMAT2 Bmax) (Fig 6 A–F). The terminal field measures tended to stay flat with respect to fiber length density until the fiber length density dropped to about 40%. At that point, almost all of the terminal field measures reached near zero. The fiber length density measure from animal 11 (shown in figure 6) was the only outlier, since it fell beyond 1.5 X interquartile range, as determined by statistical software SPSS (version 18.0.2 IBM, Chicago. IL). Striatal measures did not significantly correlate with fiber length density for the remaining animals. Fiber length density, however, did correlate with DAT density (Spearman: r = 0.81, $p < 0.001$, n = 16) (Fig 7A) and with nigral cell counts (Pearson: r = 0.66, $p = 0.01$, n = 14 with monkey 11 excluded) (Fig 7B). Fiber length density was the only striatal measure that linearly correlated with motor ratings (Spearman: r = −0.81, $p < 0.001$, n = 16) (Fig 7C).

3. Discussion

In this study we quantified terminal field and axonal response to varying degrees of MPTP-induced nigrostriatal injury. We compared new stereological measures of striatal fiber length and DAT density as determined by immunostaining with previous *in vivo* and *in vitro* measures of terminal field integrity, stereologic nigral cell counts, and ratings of motor parkinsonism from the same animals. The new findings and analyses demonstrate that *in vivo* and *in vitro* measures of striatal terminal fields correlate with each other regardless of the method of measurement. PET-based *in vivo* striatal measures accurately reflect *in vitro* measures of DAT and VMAT2. Terminal arbor size and other terminal field measures correlated with nigral cell counts only when nigral TH-ir cell loss does not exceed 50%. Interestingly the fiber length density, a measure of axonal integrity, did not correlate with striatal terminal field measures including PET measures of striatal uptake of presynaptic markers, but correlated significantly with motor ratings of parkinsonism. Thus, the new data on fiber length density measures, representing axonal integrity, fall between the striatal terminal field and nigral cell body measures.

The use of the uninjected side of the brain as control for different measurements allows us to minimize the effect of biological variability among animals. We previously published that striatal dopamine content of the uninjected side of the monkeys after unilateral MPTP infusion did not significantly differ from that of control monkeys (no MPTP infusion) (Tabbal et al., 2006; Tabbal et al., 2012). Second, we also published that the stereologic nigral counts of the uninjected side of the monkeys infused with MPTP did not significantly differ from that of control monkeys, although there is normal side-to-side variability in control monkeys (Tabbal et al., 2012).

PET-based *in vivo* striatal measures accurately reflect *in vitro* measures of DAT and VMAT2. We now show that in *vivo* PET measures of striatal BP_{ND} of CFT tightly correlate with *in vitro* quantitative autoradiographic measures of DAT B_{max} and with DAT varicosities identified with immunohistochemical labeling. Similarly, *in vivo* PET measures of striatal BP_{ND} of DTBZ tightly correlated with *in vitro* quantitative autoradiographic measures of VMAT2 B_{max} confirming that the *in vivo* PET measures accurately reflect *in vitro* VMAT2 specific binding sites. These findings are in agreement with previous studies demonstrating that PET-based estimates of VMAT2 and DAT agree well with *in vitro* autoradiographical measures of DAT and VMAT in a unilateral 6-hydroxydopamine (6-OHDA) lesioned rat model (Topping et al., 2010) and in 5 chronically MPTP-treated monkeys (Chen et al., 2008). However, our study substantially extends these studies by including a broader range of nigral cell loss severity (16–94% reduction in 15 monkeys). This ensures that our results reflect a full range of dopaminergic denervation. Interestingly, our results also agree well with previous studies using ^{18}F-FECNT, another PET radioligand for DAT, to estimate the degree of striatal and nigral dopaminergic denervatation in MPTP-treated monkeys (Masilamoni et al., 2010; Masilamoni et al., 2011). The authors reported that the ^{18}F-FECNT binding potential of the ventral midbrain and striatal regions correlates with nigral dopaminergic neurons and striatal DAT or TH immunoreactivity measurements made in 6 monkeys. Thus, these striatal PET measures can be a faithful biomarker of nigrostriatal terminal fields, but not necessarily of nigral cell bodies (Karimi et al., 2013).

Terminal arbor size expressed as the ratio between striatal terminal field (DAT varicosities) and their nigral cell bodies was not constant. Terminal arbor size decreased as more nigral cells were lost; however, once the nigral cell loss exceeded 50%, the terminal arbor size remained constant. This observation could be due to a relatively greater decline of striatal terminal fields compared to nigral loss at more severe levels of nigrostriatal injury. This supports previous reports of discordant changes in terminal fields versus nigral cell bodies in the nigrostriatal pathway in PD patients (Burke and O'Malley, 2013; Fuente-Fernandez et al., 2011; Kordower et al., 2013) and MPTP treated animals (German et al., 1996; Lavoie and Parent, 1991). Yet, these findings seem to differ from previous non-human primate PD studies that suggest terminal regeneration commences within 4 or 5 weeks in animals with partial lesions induced by MPTP as revealed by increased branching and diameter of some TH-ir fiber types (Song and Haber, 2000) or increased optical density measures of immunostaining and visual quantification of individual fibers (Mounayar et al., 2007). The differences between our findings and those from other groups may be due to the difference in monkey species, MPTP administration method, as well as the quantification method. While we used stereology for nigral cell counting, dividing striatal tissue for measurements that required fresh frozen tissue (e.g., dopamine measures and autoradiography) versus fixed tissue (immunohistochemistry) hampered the usual approach of using a random series of every n^{th} slice through the entire striatum for true stereology. Rather, we selected comparable sections of striatum from both sides of the brain and used the uninjected side as control (Brooks et al., 1987; Tabbal et al., 2006). Studies in 6-OHDA-lesioned rodents have shown that DAT varicosities in the striatum decreased up to 80% 4 weeks after lesioning but returned to normal by 16 weeks, unless nigral neuron loss were greater than 75% (Stanic et al., 2003a; Stanic et al., 2003b; Finkelstein et al., 2000). This difference might result from the differences in brain connectivity, structural complexity and behaviors between rodents and primates, including human (Jakowec and Petzinger, 2004). For example, the caudate and putamen in primates are well delineated and separated by the internal capsule; in contrast, the caudate and putamen in rodents have no clear delineation (Capitanio and Emborg, 2008). Another difference between our study and others is that we followed our animals for only two months after MPTP. This could be too short to identify compensatory changes, however we have found no evidence of functional compensation as our animal model maintains stable motor parkinsonian ratings for as long as 1.5 years (Perlmutter et al., 1997).

Fiber length density measures do not appear to mimic striatal terminal field measures. Most of the comparisons of fiber length density with either *in vitro* or *in vivo* terminal field measures (Figure 6 A–F) seem to have relatively little change until fiber length density reaches about 60% loss (0.40 ratio in the figures) and then these terminal fields measures drop to near zero. This dichotomous relationship between fiber length density and other striatal field measures was also seen in PD patients: those with less than 3 years duration of disease had a 35–75% variable loss of TH fibers in dorsal putamen, whereas loss was virtually complete for those living 5 years after diagnosis, and no further loss in those with more severe parkinsonism that lived much longer (Kordower et al., 2013). The relatively stable level of fiber length density for monkeys with 60% or more loss suggest that loss of striatal dopaminergic functions, at least as evidenced by TH staining, is largely complete by

this point. Striatal DAT density measured with immunohistochemistry (Figure 7A) may be different but that requires confirmation with more data. However, it remains uncertain whether the loss of striatal fiber density is due to fiber degeneration or a functional change in dopamine synthetic enzymes in those fibers. Interestingly, fiber length density is the only other measure that correlated with motor ratings. Thus, fiber length density does not respond to nigrostriatal injury in the same way as terminal fields but rather the degree of damage lies between the severity found in terminal fields and nigral cell bodies. Therefore, loss of terminal fields may not be the only factor that contributes to severity of parkinsonism in this animal model since parkinsonism correlates well with nigral cell counts (Tabbal et al., 2012) and nearly as well with fiber length density but not with other terminal field measures.

The conclusions based on fiber length density and DAT density measurements should be treated with caution. Interpretation of the density calculations assumes that shrinkage of tissue is the same on both sides. This may or may not be true since MPTP may cause differential shrinkage of the two striata (Yin et al., 2009) but that would most likely make the residual fibers seem more densely packed on the injected side. Yet, we did not find increased fiber density on the injected side. However, tissue preparation also could affect the MPTP side differently with potentially excessive swelling during tissue preparation thereby causing some ambiguity in interpretation despite making the measurements in the same volume of tissue on both sides (Braendgaard and Gundersen, 1986).

Our goal in this study was to perform *in vitro* quantification of MPTP-induced damage to various parts of nigrostriatal projections and to correlate those with *in vivo* PET and behavioral measures. We applied unbiased stereology to quantify the MPTP-induced damage to nigral cell bodies (TH-staining for counting the number of neurons), striatal axons (TH-staining for fiber length density) and terminal fields (DAT staining for varicosity density and terminal arbor size). These different immunohistological measurements based on stereological methods yield accurate and precise estimation of three functional aspects of the nigrostriatal pathway after MPTP-induced injury that may provide important measures for changes that occur in PD in humans. Striatal fiber measures overlap to some degree with terminal field measures but the clear distinction between the relationship of the fiber density measures with motor behavior (closer to the relationship found between nigral cell counts and behavior) compared to the limited relationship between terminal field measures and behavior (in which there is a major flooring effect after loss of half of the nigral cell bodies) supports the notion that these represent different functional components of the nigrostriatal pathway. The close correlation between the terminal field measures and striatal dopamine concentration further supports this interpretation. Technically, estimation of striatal fiber length density has been achieved through the application of virtual probes to relatively thick tissue sections; this approach allows a morphologically-based measure of the extent of dopaminergic innervations of striatum (Calhoun and Mouton, 2000). Finally, the stereological estimates of striatal DAT-ir varicosities and terminal arbor size provide a reasonable estimation of the number of terminals arising from each SNpc TH-ir neuron (Finkelstein et al., 2004). It is crucial to measure these three aspects separately as injury to each component can carry different course and consequences, and each of these components may have different responses to interventions. These findings based on these measurements

allow us to better understand the MPTP model and to accurately interpret the *in vivo* PET measures and their limitations.

The nonhuman primate model provides the anatomical connectivity and structural complexity homologous to human brain and offers several advantages for this type of study. Indeed, the unilateral infusion strategy permitted use of an internal control thereby minimizing the effects of inter-subject variability. As we previously demonstrated, striatal dopamine content and stereological nigral TH-ir neuron count of the contralateral side (uninjected side) of the monkeys infused with MPTP were not significantly different from that of the control monkeys (no MPTP infusion) (Tabbal et al., 2006; Tabbal et al., 2012). The major limitation of the acute MPTP model is that the pathophysiology of MPTP-induced nigrostriatal damage is not the same as that occurs in idiopathic PD (Jakowec and Petzinger, 2004). For example, the distribution of the striatal lesion after unilateral, single dose of MPTP (whether high or low dose) is uniform and not heterogenous as seen in human PD. We have previously reported that caudate and putamen have equal loss of dopamine (Tabbal et al., 2006; Tabbal et al., 2012) in this unilateral model. Thus, conservatively one could view MPTP as primarily a model of nigrostriatal dopaminergic cell loss rather than as a model of the pathophysiology of human PD. Hence, this model is well-suited for the purpose of this study, to compare motor parkinsonism with the degree of injury to specific components of the nigrostriatal pathway. It is important to note that the pathophysiology of nigrostriatal injury caused by unilateral MPTP infusion in monkeys differs from that in PD patients, thus limiting a direct comparison of these data to the neuropathologic changes in PD.

In summary, we found that nigrostriatal terminal field measures whether done *in vitro* or *in vivo* PET correlated with each other but that these measures did not correlate with nigral cell body counts. However, fiber length density fell between the terminal field and nigral cell counts. Yet, motor parkinsonism correlated only with striatal fiber length density. These differential effects have important implications for interpretation of neuroimaging biomarkers of nigrostriatal pathways.

4. Experimental Procedure

4.1 Ethics statement

We used the minimum number of animals necessary for this research; and all animal work has been conducted according to relevant national and international guidelines. In accordance with the recommendations of the Weatherall report, “The use of non-human primates in research”, the following statement to this effect has been included to document the details of animal welfare and steps taken to ameliorate suffering in all work involving non-human primates: this work was conducted at the Nonhuman Primate Facility of the Washington University in St. Louis with permission from its Institutional Animal Care and Use Committee (IACUC). The protocol number is 20110161, approved on 6/25/2013. The welfare of the animals conformed to the requirements of National Institutes of Health (NIH). All animals were housed in cages exceeding the stipulated sizes requirements. Animals were maintained in large group houses under 12-hour dark and light cycles, and were given access to food and water ad libitum; all animals were provided environmental enrichment such as

watching movies or playing with appropriate toys to prevent inappropriate deprivation. No animal was physically harmed or knowingly exposed to potential infection. In the event there would be mild to moderate pain discomfort: we treat with Buprenex, 0.01–0.03mg/kg for up to 3 days, per the discretion of the staff veterinarian. Humane endpoints were pre-defined in this protocol and applied as a measure of reduction of discomfort.

4.2 Subjects

Sixteen male macaques (mean age = 5.4±1.0) were studied. All 16 monkeys completed the study and demonstrated a wide range of severity of parkinsonism from none in controls to severe unilateral parkinsonism with the highest doses of MPTP (Tabbal et al., 2012). All routine animal care procedures were described in detail (Tian et al., 2012).

4.3 Protocol

Detailed descriptions of the approaches have been published earlier (Brown et al., 2012; Karimi et al., 2013; Tabbal et al., 2012; Tian et al., 2012). The following is a short overview. Each monkey had a brain magnetic resonance imaging (MRI) and baseline PET scans using FD, DTBZ, and CFT. Animals were trained to perform several behavioral tasks to assess motor ability, behavioral sessions were recorded; the behavioral data have been reported in a separate paper (Tabbal et al., 2012). A variable dose of MPTP (0–0.31 mg/kg) was infused into right internal carotid artery (Tabbal et al., 2006; Tabbal et al., 2012). Eight weeks later, two PET scans were repeated with each of the tracers. Following the final PET, the animal was euthanized with a lethal overdose of pentobarbital (100 mg/kg, i.v.) (Butler Schein Animal Health, Dublin, OH) and the brain was rapidly removed and processed as previously reported to obtain stereologic counts of nigral dopaminergic neurons, high performance liquid chromatography (HPLC) -based measures of striatal dopamine and in *vitro* quantitative autoradiography measure of DAT and VMAT2 specific binding sites (Tian et al., 2012). The time period of eight weeks after MPTP to euthanize the animals was based on previous studies showing all MPTP-treated monkeys reached maximal parkinsonian scores about 3 weeks after MPTP and their parkinsonism scores remained stable until euthanasia (Tabbal et al., 2012; Tabbal et al., 2006). A blinded reviewer rated parkinsonism on video recordings using validated scales, and the final parkinsonism score was used for analysis, as motor impairment was stable for at least 4–5 weeks prior to euthanasia (Tabbal et al., 2012; Tabbal et al., 2006; Perlmutter et al., 1997). Images were processed as previously described (Brown et al., 2012; Tabbal et al., 2006; Karimi et al., 2013). A reviewer unaware of MPTP dose manually placed the region of interests (ROIs) on the dorsal caudate nucleus and dorsal putamen on the T1-weighted magnetization prepared rapid gradient echo (MPRAGE) scan for each animal (Fig 8). The occipital cortex was used as a reference region devoid of specific binding sites and comprised of a pair of hemi-cylinders on either side of the midline in occipital cortex. The MPRAGE was coregistered to the target PET scan of that animal using a vector gradient method (Rowland et al., 2005), and the traced ROIs were transformed into PET space using the same transformation matrix.

PET analyses were done to obtain the BP_{ND} for CFT, and DTBZ according to the tissue reference method (Logan et al., 1996) using data from 30–115 min and 15–60 min after injection, respectively. We also calculated the *K*occ (influx constant using an occipital

region for the input function) for FD (Logan et al., 1996; Patlak and Blasberg, 1985) using data from 24–94 min after injection. The BP_{ND} for CFT and DTBZ and *K*occ for FD were calculated for the dorsal striatum (caudate plus putamen). Animals were always able to care for themselves and received no dopaminergic drugs at any time.

4.4 Striatal tissue

An equivalent mid section of fresh striatum was removed from both hemispheres for dopamine measurements. Fixed striatal tissue was cut coronally with a freezing microtome into 50 μm thick slices including caudate and putamen of the same hemisphere. Due to the missing tissue (fresh frozen tissue used for neurochemistry) we could not select a random series of every n^{th} slice and therefore could not calculate an absolute value for volume, total fiber length of TH stained fibers or the number of DAT-ir axonal varicosities. However, to ensure reliable right-left ratio calculations we selected 5–10 slices with similar size and location of caudate and putamen from both sides.

4.5 TH and DAT immunohistochemistry for striatum

TH immunohistochemistry was performed to label striatal fibers. The protocol was the same as for midbrain staining (Tian et al., 2012) except for the higher concentration 1:125 of TH antibody. DAT immunohistochemistry was performed to label dopaminergic terminals on a second intercalated series of striatal slices from the same tissue blocks. The immunohistochemical procedure for DAT was the same as for TH staining in midbrain but with rabbit anti-DAT (Millipore, Temecula, CA) diluted to a concentration of 1:1000.

4.6 Striatal measures

We used an Olympus BX41 Microscope (equipped with a 100 x objective with a numerical aperture of 1.3) with a Proscan stage kit and a DP70 digital camera (12 megapixel) with newCAST™ software (version 3.2.10.0; Visiopharm, Hoersholm, Denmark) to determine the striatal total fiber length density (Mouton et al., 2002; Calhoun and Mouton, 2000) and DAT density (Finkelstein et al., 2004) with comparable sampling from the two sides of the brain.

Striatal fiber length density—We used the atlas by Saleem and Logothetis (Saleem and Logothetis, 2012) to define the caudate and putamen following their anatomical outline using a 10x objective. Isotropic virtual planes were used to estimate the total fiber length in caudate and putamen slices (Calhoun and Mouton, 2000; Larsen et al., 1998). The top guard zone was set at 1 μm. To determine the volume in which the fibers were measured we used a 1% meander sampling with Cavalieri principle-based on point counting (Gundersen and Jensen, 1987). A meander sampling of 0.36% was used for fiber length estimation. Two different counting frames were used for fiber length measurement based on the severity of the fiber loss and the staining penetration. We used a counting frame with a height of 3 μm and a plane distance of 30 μm in the unaffected sides with high fiber density. Coefficients of error were the same irrespective of counting frames. To obtain fiber length density the total fiber length was divided by the volume of the sampled area. The difference in counting frames was considered in calculating the right-left ratios.

Striatal axonal varicosity count—We implemented the fractionator design for estimating the number of DAT-ir axonal varicosities (Finkelstein et al., 2004). The volume of caudate and putamen sampled was measured as above; a meander sampling of 1% was chosen for the volume estimation. Counts of DAT-ir varicosities, identified as a dilated round or oval shaped structures on immunolabeled axons (Finkelstein et al., 2004), were made using computer- assisted random sampling with a meander sampling of 0.1%. A counting frame (frame area, 30x30 μm^2; height of 3 μm; top guard zone of 1 μm) was focused through the section. The density of DAT varicosity was calculated as the total DAT varicosities divided by the volume of the sampled area.

4.7 Unbiased stereologic counting of nigrostriatal neurons

Unbiased stereological counts of nigrostriatal neurons were done on TH-immunostained midbrain slices, as previously described (Tian et al., 2012; Brown et al., 2012) The substantia nigra pars compacta (SNpc) was defined as the region ventral to the medial leminiscus and lateral to the third cranial nerve fibers; the SNpc started caudal to the hypothalamus and extended caudally to the decussation of the superior cerebral peduncle. newCAST™ was utilized to achieve random sampling of 5.22% (frame length/step length) of the total ROI area to reduce intra-sectional variance with an 80 × 80 μm^2 counting frame and height of 22 μm with a 3 μm top guard zone. Only TH-positive neurons were counted as long as a nucleus could be distinguished. Counting was performed on equidistant slices throughout the extent of the structures, which reduces inter-sectional variance. An injected/control side ratio was calculated from cell counts for each subject.

4.8 Data analysis and Statistics

We calculated a ratio of injected to control side to account for inter-subject variations. Results were analyzed using SPSS. The average terminal arbor size of the MPTP lesioned side was expressed as a ratio of striatal DAT varicosities (injected to control ratio) to nigral cell count (injected to control ratio) (Lee et al., 2008). Relationships between variables were calculated using either Spearman or Pearson correlations, where appropriate based upon distribution of data or data type (analysis of rating scale relationships was done with Spearman). A two-tailed *P* value of less than 0.05 was considered significant.

Acknowledgments

We thank Hubert P Flores, Christina Zukas, Darryl Craig, and Terry Anderson for expert technical assistance.

Reference List

Bankiewicz KS, Oldfield EH, Chiueh CC, Doppman JL, Jacobowitz DM, Kopin IJ. Hemiparkinsonism in monkeys after unilateral internal carotid artery infusion of 1-methyl-4-phenyl-1,2,3,6-tetrahydropyridine (MPTP). Life Sci. 1986; 39:7–16. [PubMed: 3487691]

Braendgaard H, Gundersen HJ. The impact of recent stereological advances on quantitative studies of the nervous system. J Neurosci Methods. 1986; 18:39–78. [PubMed: 3540470]

Brooks BA, Eidelberg E, Morgan WW. Behavioral and biochemical studies in monkeys made hemiparkinsonian by MPTP. Brain Res. 1987; 419:329–332. [PubMed: 3499952]

Brown CA, Campbell MC, Karimi M, Tabbal SD, Loftin SK, Tian LL, Moerlein SM, Perlmutter JS. Dopamine pathway loss in nucleus accumbens and ventral tegmental area predicts apathetic behavior in MPTP-lesioned monkeys. Exp Neurol. 2012; 236:190–197. [PubMed: 22579525]

Burke RE, O'Malley K. Axon degeneration in Parkinson's disease. Exp Neurol. 2013; 246:72–83. [PubMed: 22285449]

Calhoun ME, Mouton PR. Length measurement: new developments in neurostereology and 3D imagery. Journal of Chemical Neuroanatomy. 2000; 20:61–69. [PubMed: 11074344]

Capitanio JP, Emborg ME. Contributions of non-human primates to neuroscience research. Lancet. 2008; 371:1126–1135. [PubMed: 18374844]

Chen MK, Kuwabara H, Zhou Y, Adams RJ, Brasic JR, McGlothan JL, Verina T, Burton NC, Alexander M, Kumar A, Wong DF, Guilarte TR. VMAT2 and dopamine neuron loss in a primate model of Parkinson's disease. J Neurochem. 2008; 105:78–90. [PubMed: 17988241]

Finkelstein DI, Stanic D, Parish CL, Drago J, Horne MK. Quantified assessment of terminal density and innervation. Curr Protoc Neurosci. 2004; Chapter 1

Finkelstein DI, Stanic D, Parish CL, Tomas D, Dickson K, Horne MK. Axonal sprouting following lesions of the rat substantia nigra. Neuroscience. 2000; 97:99–112. [PubMed: 10877666]

Fuente-Fernandez R, Schulzer M, Kuramoto L, Cragg J, Ramachandiran N, Au WL, Mak E, McKenzie J, McCormick S, Sossi V, Ruth TJ, Lee CS, Calne DB, Stoessl AJ. Age-specific progression of nigrostriatal dysfunction in Parkinson's disease. Ann Neurol. 2011; 69:803–810. [PubMed: 21246604]

German DC, Nelson EL, Liang CL, Speciale SG, Sinton CM, Sonsalla PK. The neurotoxin MPTP causes degeneration of specific nucleus A8, A9 and A10 dopaminergic neurons in the mouse. Neurodegeneration. 1996; 5:299–312. [PubMed: 9117541]

Gundersen HJ, Jensen EB. The efficiency of systematic sampling in stereology and its prediction. J Microsc. 1987; 147:229–263. [PubMed: 3430576]

Jakowec MW, Petzinger GM. 1-methyl-4-phenyl-1,2,3,6-tetrahydropyridine-lesioned model of parkinson's disease, with emphasis on mice and nonhuman primates. Comp Med. 2004; 54:497–513. [PubMed: 15575363]

Joyce JN, Marshall JF, Bankiewicz KS, Kopin IJ, Jacobowitz DM. Hemiparkinsonism in a monkey after unilateral internal carotid artery infusion of 1-methyl-4-phenyl-1,2,3,6-tetrahydropyridine (MPTP) is associated with regional ipsilateral changes in striatal dopamine D-2 receptor density. Brain Res. 1986; 382:360–364. [PubMed: 2944565]

Karimi M, Tian L, Brown CA, Flores HP, Loftin SK, Videen TO, Moerlein SM, Perlmutter JS. Validation of nigrostriatal positron emission tomography measures: Critical limits. Ann Neurol. 2013; 73:390–396. [PubMed: 23423933]

Kordower JH, Olanow CW, Dodiya HB, Chu Y, Beach TG, Adler CH, Halliday GM, Bartus RT. Disease duration and the integrity of the nigrostriatal system in Parkinson's disease. Brain. 2013; 136:2419–2431. [PubMed: 23884810]

Larsen JO, Gundersen HJ, Nielsen J. Global spatial sampling with isotropic virtual planes: estimators of length density and total length in thick, arbitrarily orientated sections. J Microsc. 1998; 191:238–248. [PubMed: 9767488]

Lavoie B, Parent A. Dopaminergic neurons expressing calbindin in normal and parkinsonian monkeys. Neuroreport. 1991; 2:601–604. [PubMed: 1684519]

Lee J, Zhu WM, Stanic D, Finkelstein DI, Horne MH, Henderson J, Lawrence AJ, O'Connor L, Tomas D, Drago J, Horne MK. Sprouting of dopamine terminals and altered dopamine release and uptake in Parkinsonian dyskinaesia. Brain. 2008; 131:1574–1587. [PubMed: 18487277]

Logan J, Fowler JS, Volkow ND, Wang GJ, Ding YS, Alexoff DL. Distribution volume ratios without blood sampling from graphical analysis of PET data. J Cereb Blood Flow Metab. 1996; 16:834–840. [PubMed: 8784228]

Masilamoni G, Votaw J, Howell L, Villalba RM, Goodman M, Voll RJ, Stehouwer J, Wichmann T, Smith Y. (18)F-FECNT: validation as PET dopamine transporter ligand in parkinsonism. Exp Neurol. 2010; 226:265–273. [PubMed: 20832405]

Masilamoni GJ, Bogenpohl JW, Alagille D, Delevich K, Tamagnan G, Votaw JR, Wichmann T, Smith Y. Metabotropic glutamate receptor 5 antagonist protects dopaminergic and noradrenergic neurons from degeneration in MPTP-treated monkeys. Brain. 2011; 134:2057–2073. [PubMed: 21705423]

Mounayar S, Boulet S, Tande D, Jan C, Pessiglione M, Hirsch EC, Feger J, Savasta M, Francois C, Tremblay L. A new model to study compensatory mechanisms in MPTP-treated monkeys exhibiting recovery. Brain. 2007; 130:2898–2914. [PubMed: 17855373]

Mouton PR, Gokhale AM, Ward NL, West MJ. Stereological length estimation using spherical probes. J Microsc. 2002; 206:54–64. [PubMed: 12000563]

Palombo E, Porrino LJ, Bankiewicz KS, Crane AM, Sokoloff L, Kopin IJ. Local cerebral glucose utilization in monkeys with hemiparkinsonism induced by intracarotid infusion of the neurotoxin MPTP. J Neurosci. 1990; 10:860–869. [PubMed: 2319306]

Patlak CS, Blasberg RG. Graphical evaluation of blood-to-brain transfer constants from multiple-time uptake data. Generalizations. J Cereb Blood Flow Metab. 1985; 5:584–590. [PubMed: 4055928]

Perlmutter JS, Tempel LW, Black KJ, Parkinson D, Todd RD. MPTP induces dystonia and parkinsonism. Clues to the pathophysiology of dystonia. Neurology. 1997; 49:1432–1438. [PubMed: 9371934]

Rowland DJ, Garbow JR, Laforest R, Snyder AZ. Registration of [18F]FDG microPET and small-animal MRI. Nucl Med Biol. 2005; 32:567–572. [PubMed: 16026703]

Saleem, KS.; Logothetis, NK. A combined MRI and histology atlas of the rhesus monkey brain in stereotaxic coordinates. Academic Press; 2012.

Song DD, Haber SN. Striatal responses to partial dopaminergic lesion: evidence for compensatory sprouting. J Neurosci. 2000; 20:5102–5114. [PubMed: 10864967]

Stanic D, Finkelstein DI, Bourke DW, Drago J, Horne MK. Timecourse of striatal re-innervation following lesions of dopaminergic SNpc neurons of the rat. Eur J Neurosci. 2003a; 18:1175–1188. [PubMed: 12956716]

Stanic D, Parish CL, Zhu WM, Krstew EV, Lawrence AJ, Drago J, Finkelstein DI, Horne MK. Changes in function and ultrastructure of striatal dopaminergic terminals that regenerate following partial lesions of the SNpc. J Neurochem. 2003b; 86:329–343. [PubMed: 12871574]

Tabbal SD, Mink JW, Antenor JA, Carl JL, Moerlein SM, Perlmutter JS. 1-Methyl-4-phenyl-1,2,3,6-tetrahydropyridine-induced acute transient dystonia in monkeys associated with low striatal dopamine. Neuroscience. 2006; 141:1281–1287. [PubMed: 16766129]

Tabbal SD, Tian L, Karimi M, Brown CA, Loftin SK, Perlmutter JS. Low nigrostriatal reserve for motor parkinsonism in nonhuman primates. Exp Neurol. 2012; 237:355–362. [PubMed: 22836146]

Tian L, Karimi M, Loftin SK, Brown CA, Xia H, Xu J, Mach RH, Perlmutter JS. No Differential Regulation of Dopamine Transporter (DAT) and Vesicular Monoamine Transporter 2 (VMAT2) Binding in a Primate Model of Parkinson Disease. PLoS One. 2012; 7:e31439. [PubMed: 22359591]

Topping GJ, Dinelle K, Kornelsen R, McCormick S, Holden JE, Sossi V. Positron emission tomography kinetic modeling algorithms for small animal dopaminergic system imaging. Synapse. 2010; 64:200–208. [PubMed: 19862685]

Yin D, Valles FE, Fiandaca MS, Forsayeth J, Larson P, Starr P, Bankiewicz KS. Striatal volume differences between non-human and human primates. J Neurosci Methods. 2009; 176:200–205. [PubMed: 18809434]

Highlights

- Fiber length density of nigrostriatal neurons correlate with motor parkinsonism.
- Motor parkinsonism does correlate with dopaminergic nigral neuron counts.
- Motor parkinsonism does not correlate with striatal dopamine.
- Several *in vivo* and *in vitro* measures of striatal terminal fields correlate with each other.
- PET-based striatal measures of DTA and VMAT2 accurately reflect corresponding *in vitro* measures.

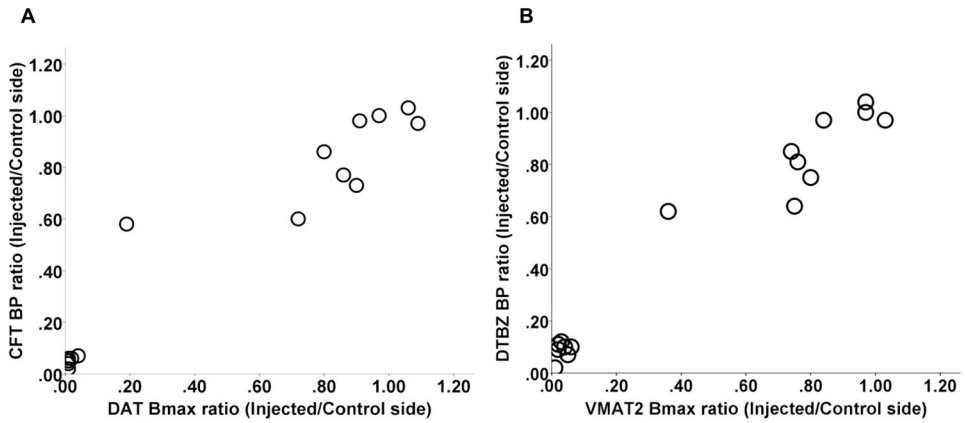

Figure 1.

In vivo PET data had a tight correlation with corresponding *in vitro* measures. CFT BP_{ND} tightly correlated with DAT Bmax (A); striatal DTBZ BP_{ND} correlated strongly with VMAT2 Bmax (B). The value for each monkey was expressed as the ratio of the injected side to the control side.

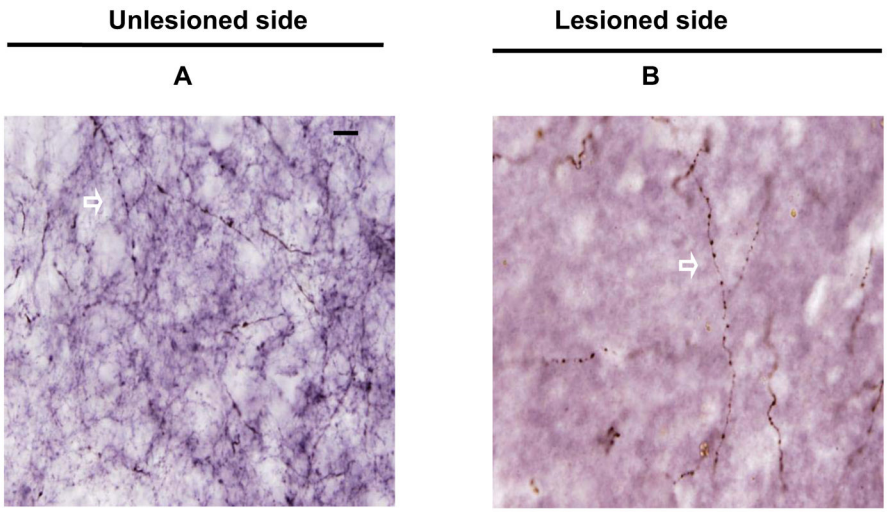

Figure 2.

Representative coronal sections of post-commissural striatum showing dopamine transporter (DAT) immunoreactivity of the unlesioned side (A) and lesioned side (B) under high power (x100 objective) from a monkey given MPTP 0.25 mg/kg. The arrows indicated the DAT varicosities. Scale bar 100 μm (A and B).

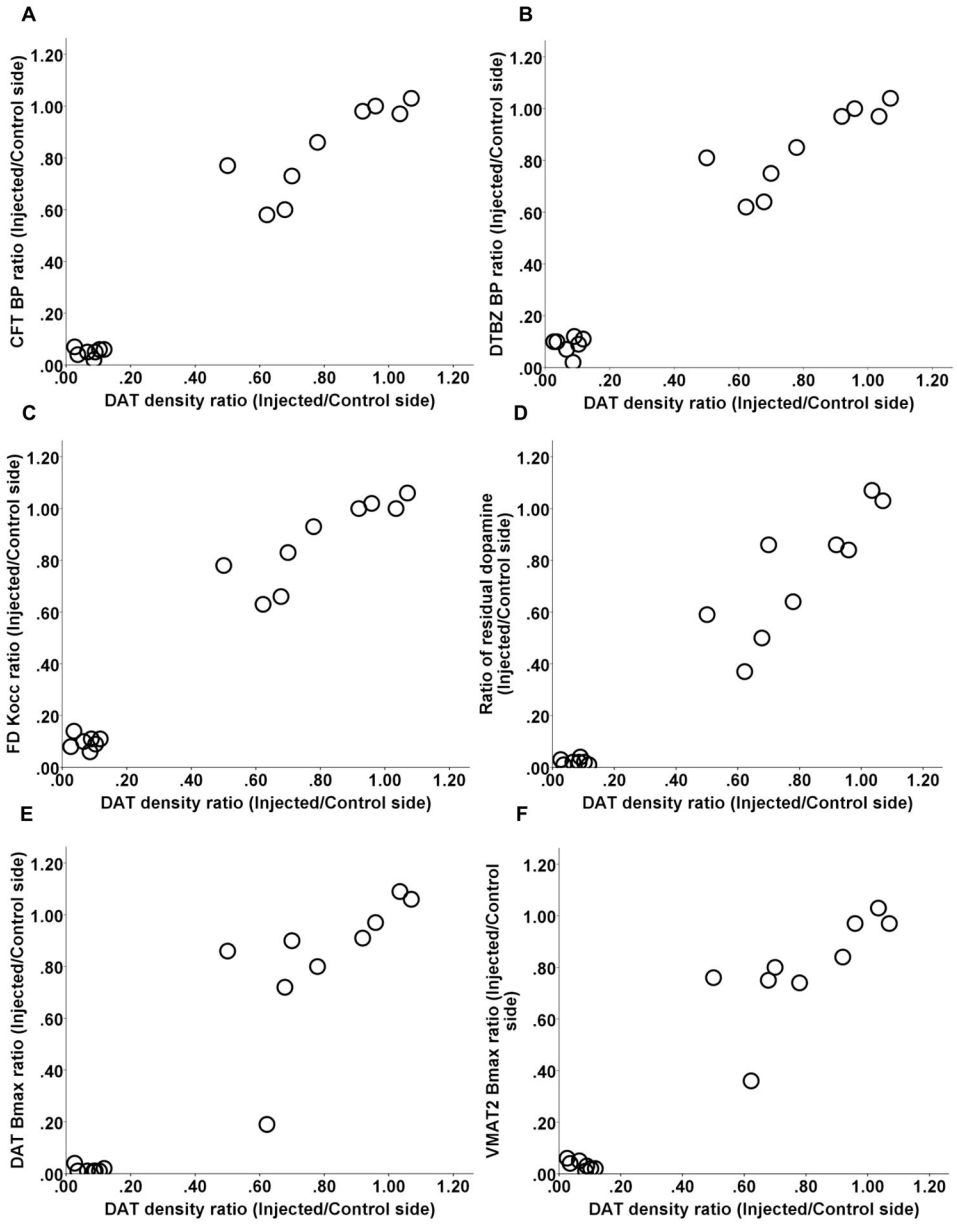

Figure 3.

Relationship between DAT density and other striatal terminal field measures including CFT BP_{ND}, DTBZ BP_{ND} and FD K_{occ}, striatal dopamine, DAT Bmax, and VMAT2 Bmax (A-F). Note, that all correlations remained significant when including only a single point in the lower left part of the graphs (Spearman: r = 0.89, $p < 0.001$; r = 0.91, $p < 0.0001$; r = 0.94, $p < 0.0001$; r = 0.92, $p < 0.0005$; r = 0.89, $p < 0.001$; r = 0.86, $p = 0.002$, respectively; n = 10).

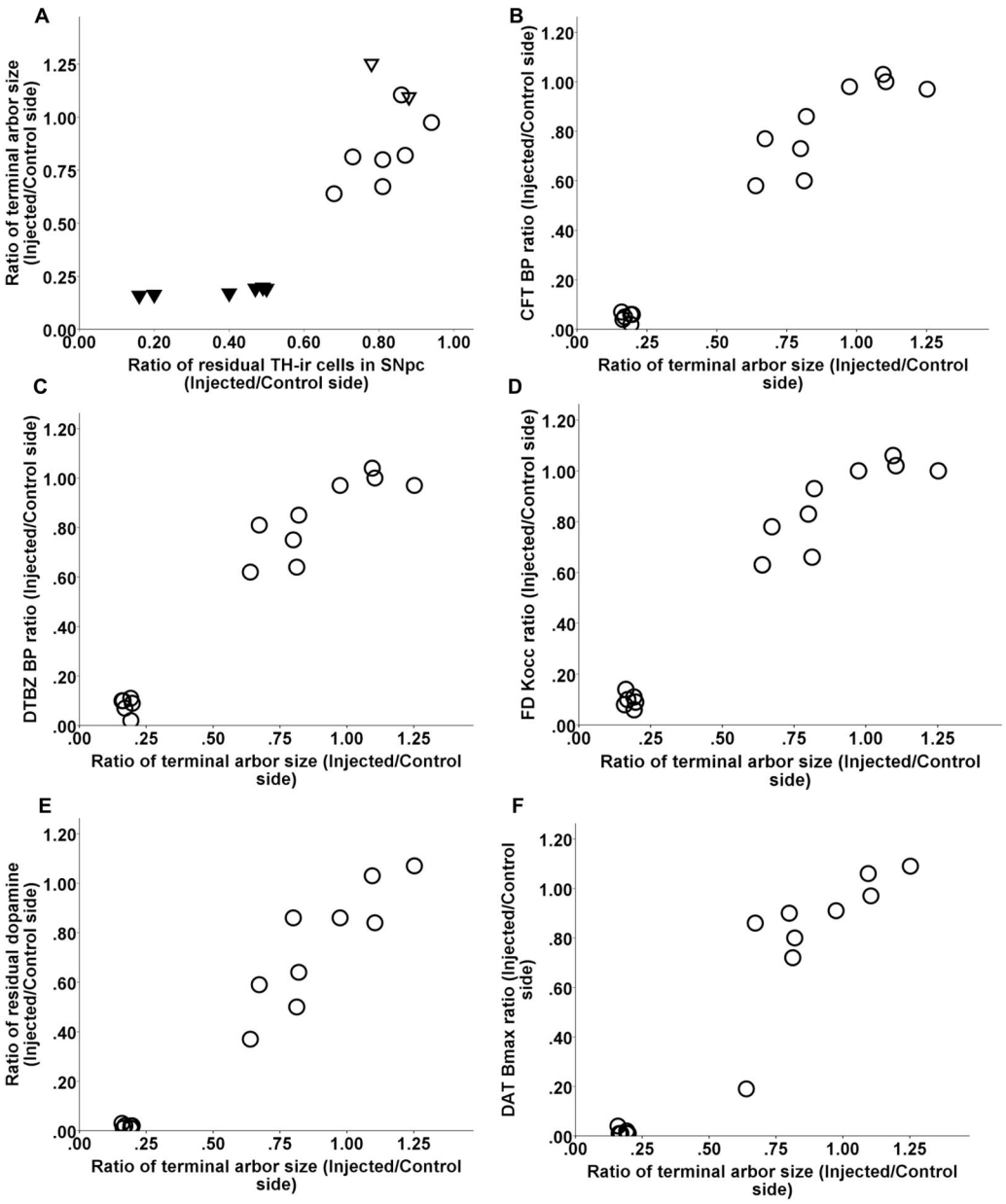

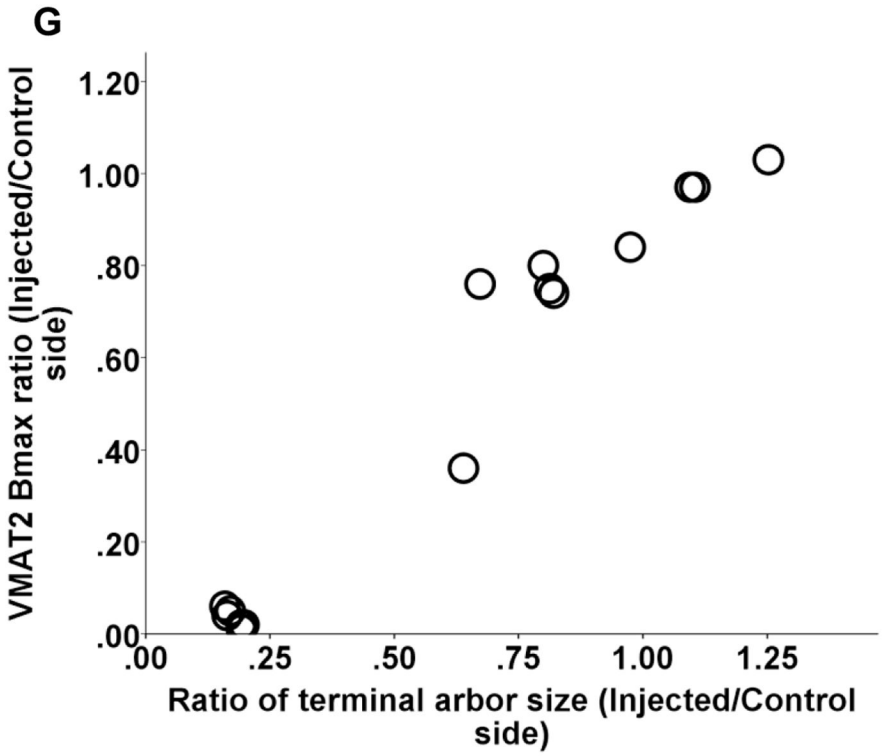

Figure 4.

Relationship between DAT terminal arbor size and nigral cell count and other striatal terminal field measures including CFT BP_{ND}, DTBZ BP_{ND} and FD K_{occ}, striatal dopamine, DAT Bmax, and VMAT2 Bmax (A–G). In figure A, the ratio of residual TH-ir cells in the substantia nigra pars compacta (SNpc) are labeled as following: control (open triangles), 16–50% (solid triangles), 51–100% (open circles). Note, that all correlations between DAT terminal arbor size and above striatal terminal field measures remained significant when including only a single point in the lower left part of the graphs (Spearman: r = 0.87, p = 0.001; r = 0.89, p = 0.001; r = 0.9, p = 0.001, r = 0.89, $p < 0.0001$; r = 0.98, $p < 0.0001$; r = 0.85, $p < 0.0001$; r = 0.92, $p < 0.0005$; respectively; n = 10).

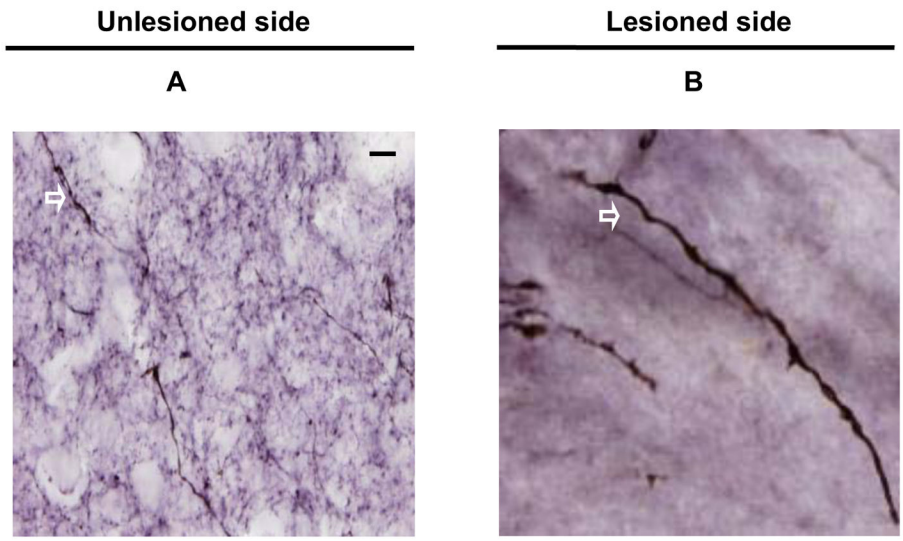

Figure 5.

Representative coronal sections of post-commissural striatum showing TH immunoreactivity of the unlesioned side (A) and lesioned side (B) under high power (x100 objective) from a monkey given MPTP 0.25 mg/kg. The arrows indicated the TH immunoreactive fibers. Scale bar = 100 μm (A and B).

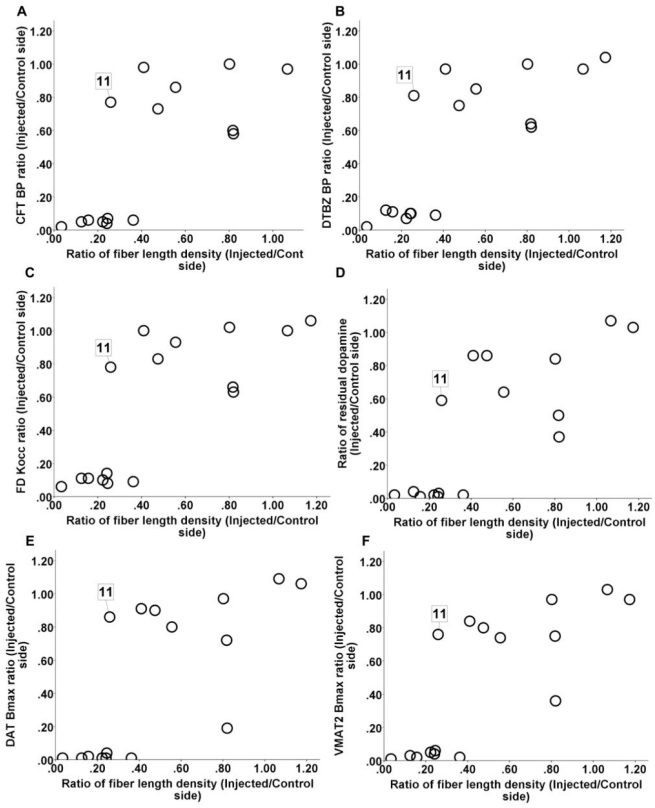

Figure 6.

The fiber length density had a dichotomous relationship with *in vitro* or *in vivo* striatal terminal field measures DAT Bmax (A), VMAT2 Bmax (B) and dopamine (C), CFT BP_{ND} (D), DTBZ BP_{ND} (E) and FD K_{occ} (F). Animal 11 is the only statistical outlier identified by SPSS defined as values below or above 1.5* interquartile range. The value for each monkey was expressed as the ratio of the injected side to the control side.

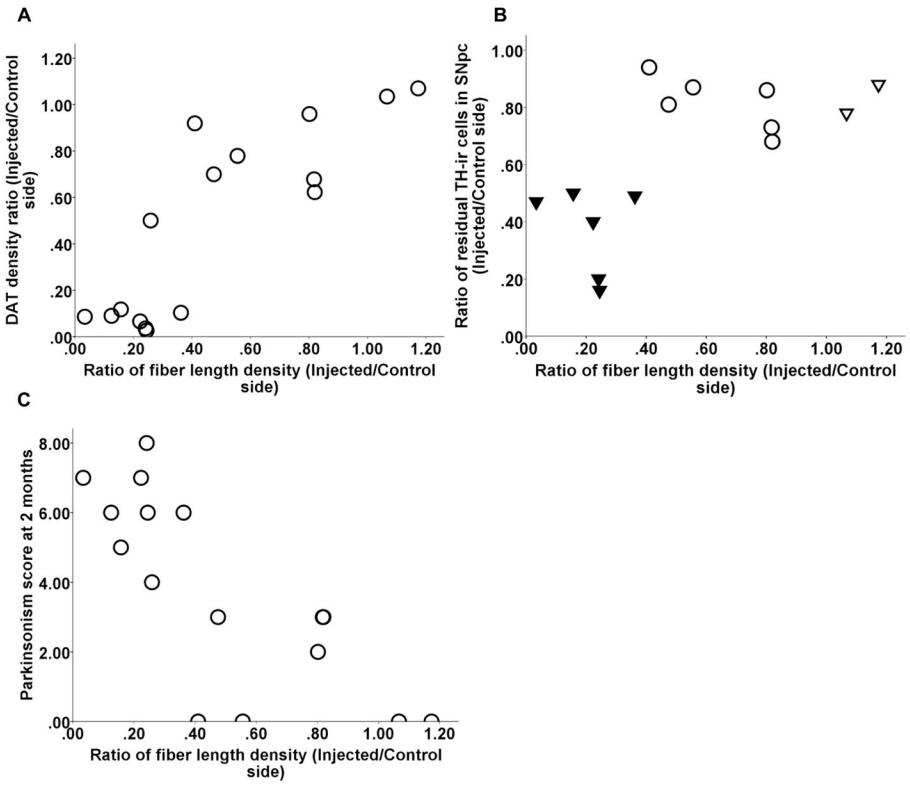

Figure 7.

Relationship between fiber length density and DAT density (A) and residual TH-ir neurons in SNpc (B). Fiber length density linearly correlated with motor ratings (C). Note, in figure B, the ratio of residual TH-ir cells in SNpc are labeled as following: control (open triangles), 16–50% (solid triangles), 51–100% (open circles). The value for each monkey was expressed as the ratio of the injected side to the control side.

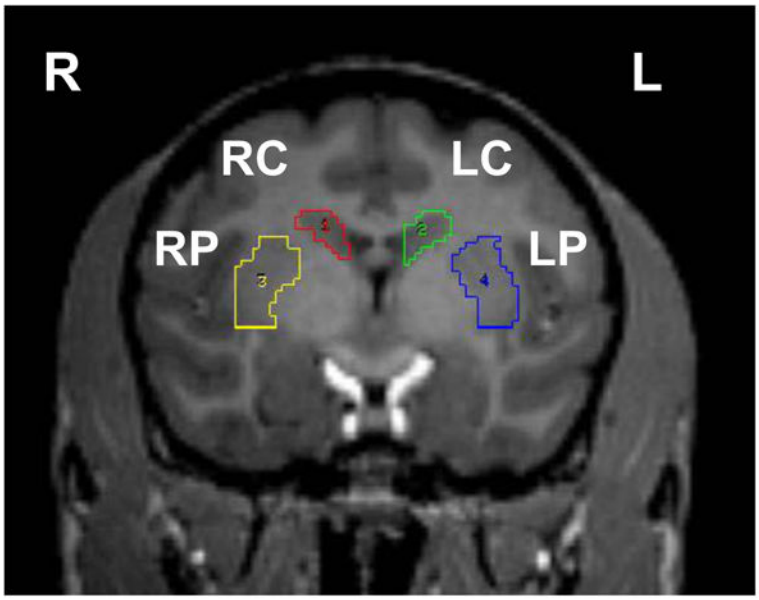

Figure 8.

The structures (regions of interest, ROI) analyzed in the right (R) and left (L) hemispheres are shown: dorsal caudate (LC, RC) and dorsal putamen (LP, RP).